DOI: 10.3969/j.issn.1673-3185.2016.02.003 **http:** // english.ship-research.com

Translated from: ZHENG Lijie, XU Jian, WU Fangliang, et al. Influences of ventilation modes on the coughing droplet dispersion process in a cruise cabin[J]. Chinese Journal of Ship Research, 2016, 11(2): 12-20.

Influences of ventilation modes on the coughing droplet dispersion process in a cruise cabin

ZHENG Lijie[1], *XU Jian*[1], *WU Fangliang*[1], *XU Wentao*[1], *LONG Zhengwei*[2]

1 China Ship Development and Design Center, Wuhan 430064, China

2 School of Environmental Science and Engineering, Tianjin University, Tianjin 300072, China

Abstract: Aiming at problem of the high infection rate of respiratory diseases on cruise ships and the corresponding lack of quantitatively research, the Computational Fluid Dynamics (CFD) method is adopted in this paper to analyze the droplet transmission and dispersion process coughed by an infected passenger accommodated in an enclosed cabin quantitatively. The air flow equation is solved by solving the unsteady Reynolds averaged Navier-Stokes equations while the Eulerian model is used to simulate the coughing droplet dispersion. The controlling effects for reducing the droplet concentration are also investigated under various conditions of changing ventilation modes and increasing ventilation rates. The results show that the displacement ventilation mode is superior to the mixed ventilation mode when increasing the ventilation rate to control the droplet dispersion. The mixed ventilation mode needs at least three air changes to empty the droplet, while the displacement ventilation mode needs only two, and the reduction of averaged droplet concentration obeys exponential distribution. In addition, the sleeping gestures of the infector have big influences on the droplet concentration in the breathing zone and inhaled dose of the susceptible.

Key words: cruise cabin; droplet dispersion; ventilation mode; numerical simulation

CLC number: U664.86

0 Introduction

The cruise industry has rapidly developed in the global leisure tourism market. In 2013, there were about 21.3 million tourists travelling by cruise ship around the world. Besides, as a mobile city, the cruise ship is becoming larger and larger and the total number of persons (including passengers and crew) in some large-scale cruise ships has been more than 3 000[1]. The fact that a large number of tourists from all over the world gather on the cruise ship (average days for a single sailing: 7 days) has brought serious challenges to the public health and safety. Since the passengers and crews spend most of their time in the "indoor" space environment such as the cruise cabin, dining room and bar and this kind of enclosed space will facilitate the spread of germs, the cruise is also known as the mobile "incubator" for disease. The infection rate of respiratory diseases is the highest on cruise ships and these diseases (e.g., influenza, diphtheria, varicella and measles) account for about 29.1% of all diseases[2]. It is generally acknowledged that the air is an important way for the transmission of respiratory diseases, which means when the infected passengers or crew conduct the respiratory behaviors such as breathing, coughing, talking and snuffing, germs of respiratory diseases which adhered to the exhaled droplet can be spread and dispersed through the air. Therefore, the germs are inhaled by other healthy persons through the respiratory tract, which makes them sick[3].

In recent years, the Computational Fluid Dynamics (CFD) has been widely used in predicting the transmission and dispersion of droplet exhaled by

Received: 2015-03-09

Supported by: Preferential Funding Program of Ministry of Human Resources and Social Security for Science and Technology Activity of Overseas Students

Author(s): ZHENG Lijie (Corresponding author), male, born in 1979, Ph. D., senior engineer. Research interests: overall ship design and fluid mechanics. E-mail: zhenglijie1979@163.com

XU Jian, male, born in 1963, Ph. D., professor. Research interests: overall ship design and fluid dynamics

people who are in the indoor space of building and the enclosed space of transportation tools. For example, He et al.[4] simulated the transmission and dispersion of droplet exhaled by people under various ventilation modes in a typical office environment. Gupta et al. [5] calculated the transmission of droplet exhaled by infected passenger who was sitting in the middle of the passenger-filled cabin of a 7-row-seat and double-aisle passenger airplane. Zhu et al.[6] conducted the numerical prediction for the transmission of influenza virus in the carriage air of the microenvironment of public buses. Zhang et al.[7] simulated the dispersion process of droplet produced by cough of a passenger in the carriage of a fully filled high-speed passenger train. However, the research of reference shows that there is little quantitative research on the transmission and dispersion process of droplet generated by respiratory behaviors of passengers in the low-rise and narrow space such as the enclosed cabin of cruise ships in China and abroad.

The effective ship ventilation system design can reduce the risk of spreading airborne pollutants and infectious diseases. Generally speaking, the cruise ships have various types of guest rooms, such as balcony cabin, ocean-view cabin, suite and inside cabin. Among them, the ocean-view cabin (because of sink-resistance requirements of cruise ships, the windows are usually enclosed and cannot be opened) and inside cabin account for a considerable proportion (Fig. 1). They are low-rise, long, narrow and enclosed. Besides, they are ventilated entirely through the machinery and cannot utilize the natural ventilation to improve the air environment inside the cabin as the balcony cabin and suite.

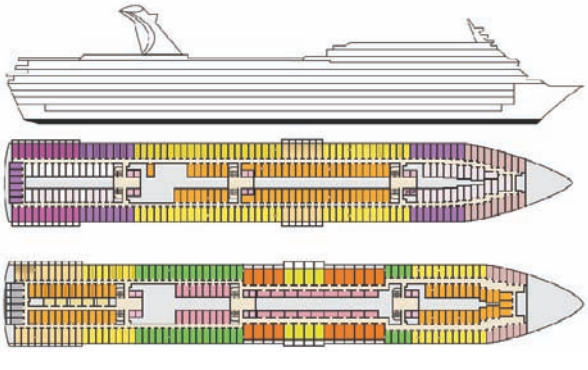

Fig.1 Typical deck plan of cabins on a cruise ship (partially)

This paper uses the CFD method to quantitatively analyze the transmission and dispersion process of coughing droplets in an enclosed cabin of a cruise ship, namely, an "indoor" space environment where the passengers stay for the longest time. It investigated the effects of increasing ventilation rates and changing ventilation modes on reducing droplet concentration, providing references for the optimization and improvement of ventilation and air conditioning system and air distribution design as well as the quantitative risk assessment of respiratory diseases.

1 Calculation method and verification

1.1 Calculation method

The dispersion of coughing droplet in the air can affect the air micro-environment of the enclosed cabin. This flow phenomenon is in fact a kind of gas-liquid two-phase flow. As for air flow, this paper adopts the method of solving the unsteady Reynolds averaged Navier-Stokes equations (URANS). As for problems of the droplet dispersion, since the coughing droplet can rapidly evaporate into the droplet nucleus of 1 μm in a very short period (< 1 s), this research ignores the transient process of droplet evaporation and at the same time the gravitational settling effects generated in the droplet dispersion process can also be ignored[8]. The droplet can be regarded as being equivalent to a passive scalar component and can be solved by Eulerian model.

The URANS equation and Eulerian model can be described as the following governing partial differential equation:

$$\frac{\partial(\rho\phi)}{\partial t}+\frac{\partial}{\partial x_j}(\rho u_j\phi)=\frac{\partial}{\partial x_j}\left(\Gamma_{\phi,\mathrm{eff}}\frac{\partial\phi}{\partial x_j}\right)+S_\phi \quad (1)$$

where ρ represents the air density; ϕ is the scalar variable which respectively represents the velocity component $u_j(x_j, j=1,2,3)$ in 3 directions of rectangular coordinate system; t denotes the time; $\Gamma_{\phi,\mathrm{eff}}$ refers to the effective diffusion coefficient; S_ϕ is the source item. Through designating different variable values of ϕ, Eq. (1) can represent the equation of continuity, momentum equation, turbulence equation, energy equation and convection diffusion equation of pollutants.

The indoor air flow is usually the turbulent flow, so turbulence mode is needed to close the Reynolds stress item of momentum equation. Compared to other eddy viscosity models, the RNG $k-\varepsilon$ turbulence model has higher precision and stability and less calculation consumption in aspects of simulating indoor air flow[9]. As a result, this research utilizes the RNG $k-\varepsilon$ turbulence model to conduct the calculation.

The dispersion of Eq. (1) adopts the finite volume

method and second-order upwind scheme. The finite volume method refers to dividing the computational domain into many grid computing units, integrating governing equations in all grid computing units and then dispersing the non-linear partial differential equation into a group of algebraic equations represented by grid nodes. The wall function of logarithmic layer is adopted to bridge the solved variables of grid units near wall and the corresponding variables on the wall. The implicit Simple algorithm is utilized to couple the pressure and velocity field. The buoyancy effects of momentum equation should be calculated by Boussinesq hypothesis, that is, assuming the buoyancy of fluid is proportional to density variations.

The convergence criteria is to reach the equilibrium state of mass and heat at the same time; the convergence residual error of energy equation is 10^{-6}; the convergence residual error of other variables is 10^{-3}.

1.2 Verification of calculation method

The method proposed by Yuan[10] is adopted to measure air flow distribution, air temperature and tracer gas concentration in a small-sized office and then the measured results are verified by the CFD calculation method (the RNG $k-\varepsilon$ turbulence model simulates the air flow and the Eulerian model stimulates the dispersion of tracer gas). It can be seen in Fig. 2 that the air flow in this office (length: 5.16 m; width: 3.65 m; height: 2.43 m) refers to the forced convection caused by integrated air supply inertial force and the mixed convection pattern of natural convection generated by heating human body and object. It is the same with the flow mode of research object presented in Section 2.1 which is described below. As a result, measurement results of this experiment are used to verify the CFD calculation method.

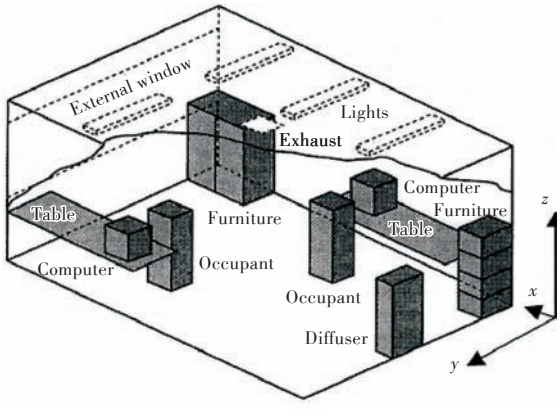

Fig.2 The office configuration used for CFD program validation[10]

In this office, 2 staff members, 2 computers and 6 lamps on the ceiling are heating elements and their total heat source power is 636 W. As tracer gas, SF6 can stimulate CO_2 exhaled by people. In addition, the displacement ventilation mode is adopted. This mode directly transmits fresh air from the bottom of the cabin to the human activity area. Since the temperature of the air supply is lower than that of indoor air, the air supply first spreads onto the floor surface under the action of gravity, then is transmitted from bottom to the top by the motivation of subsequent air supply and the entrainment and ascension function of thermal convection generated by the indoor heat source, forming a dominant air flow of indoor air movement and finally is expelled from the top of the room to the outside of cabin. All indoor air is in the stratified flow pattern and forms the indoor temperature gradient and concentration gradient in the vertical direction.

The air supply temperature of air diffuser is 17 ℃ and its air supply volume is 183 m^3/h. This diffuser possesses a porous structure and its actual effective flow area is less than its surface area. Therefore, the momentum source method[11] is adopted to set the inflow boundary condition of this diffuser, which can guarantee that the mass flow rate is consistent with the momentum flow rate at the same time. Its core concept is to adopt the rectangular opening which has the same external dimension with the original diffuser vent to replace the original one and set the momentum flow rate of the vent as M_{in} which is the actual momentum flow rate of the air. Its definition is as follows:

$$M_{in} = mv_r = m\frac{L}{A_e} = m\cdot\frac{L}{A}\cdot\frac{A}{A_e} = m\cdot\frac{L}{A}\cdot\frac{1}{f} \qquad (2)$$

where m refers to the actual mass flow rate of inflow air, kg/s; v_r is the actual flow velocity of vent, m/s; L refers to the actual inflow air quantity, m^3/s; A_e is the effective area of the vent, m^2; A is the surface area of the vent; f refers to the ratio of the effective area to surface area of vent. The momentum source method can be regarded as using countless small rectangular openings to replace the actual vent of the diffuser, so it can make sure that the inflow momentum which is an important physical parameter influencing the jet flow characteristics is consistent with the actual inflow momentum.

Fig. 3 compares the air flow distribution on the middle section of the direction y. Calculation results of CFD are similar to its measurement results, which indicates that CFD can accurately re-display the air

current circulation at the bottom of the room and meanwhile the magnitude of the airflow velocity is also consistent with measurement results. Fig. 4 lists the measurement results and calculation results of CFD for the airflow velocity, air temperature and tracer gas concentration in the middle of the office. Calculation results of CFD and measurement results of airflow velocity and air temperature match well and the temperature gradient is formed in the vertical direction; while calculation results of the tracer gas concentration can be well consistent with its measurement results at the bottom of the office but the match results are not desirable in the upper part of the office. However, CFD still calculates the concentration gradient in the vertical direction.

The comparison of calculation results of CFD and experimental results indicates that the CFD calculation method presented in Section 1.1 can accurately predict the airflow velocity, air temperature and the dispersion of pollutants in the confined space under the mixed convection mode.

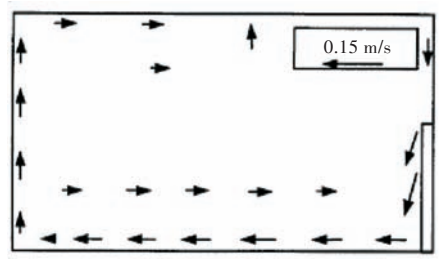

(a) Observed value in the experiment

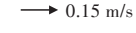

(b) Value computed by CFD

Fig.3 The airflow pattern observed by experiment[10] and computed by CFD in the mid-plane along the y-direction

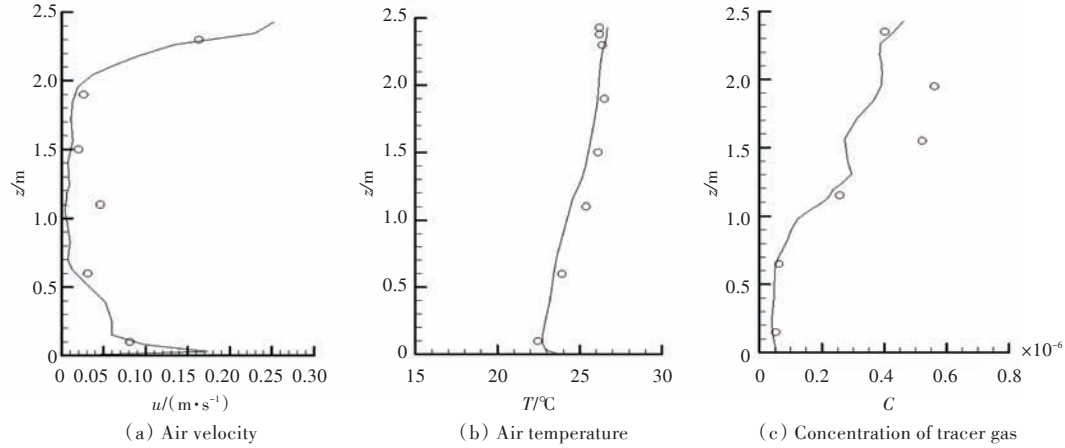

(a) Air velocity (b) Air temperature (c) Concentration of tracer gas

Fig.4 The comparison of the profiles of air velocity, air temperature and SF6 concentration between the CFD results (lines) and experimental data (circles) at the center of the office

2 Cases setting

2.1 Geometric model

Fig. 5 shows the enclosed cabin studied in this paper. The length is 3.1 m (from bow to stern), width is 5.6 m (from port to starboard) and the height is 2.15 m which is markedly lower than that of general building rooms, reflecting that it is low-rise, long, narrow, and enclosed. Four cases are calculated in total and the descriptions of these cases are shown in Table 1. The mixed ventilation mode and displacement ventilation mode both belong to mechanical ventilation mode. On the basis of dilution principle, the mixed ventilation mode sends the fresh air into the room from the top of the room to make the fresh air fully mix with the indoor air and dilute indoor pollutants.

Table 1 Case table

Case	Ventilation mode	Ventilation rate of the cabin/(Times·h^{-1})	Staff gesture
1	Mixed ventilation	8	Supine gesture
2	Mixed ventilation	12	Supine gesture
3	Displacement ventilation	8	Supine gesture
4	Mixed ventilation	8	Side lying of passenger 1

Within the cabin, there are 2 single beds on which 2 passengers sleep separately. Passenger 1 is as-

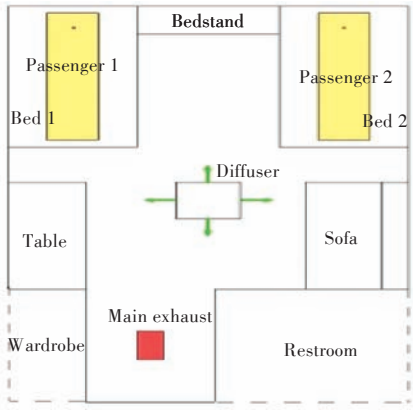

(a) Top view

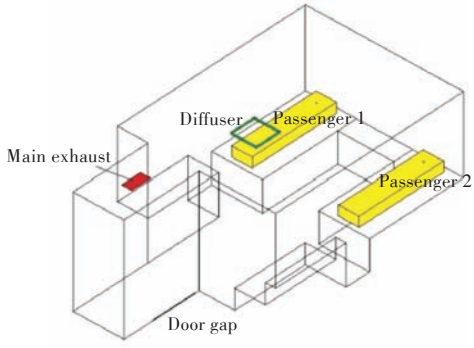

(b) Computational physical model in cases 1 and 2

Fig.5 Cabin layout

sumed to be infected, while passenger 2 is assumed to be in a state of health. Besides, there are also bedside cupboard, table, sofa, wardrobe and restroom in the cabin. Fig. 5(b) is the physical model used for the CFD calculation. This model does not include regions such as single bed, bedside cupboard, table, sofa, wardrobe and restroom that the fluid cannot reach.

The case 1 adopts the mixed ventilation mode that can input the fresh air from the top of the cabin. According to GB/T 13409-92[12], the air change per hour (*ACH*) of the cabin is 8 times/h, which means that theACH equals 8. The length and height of each supply vent of the four-directional diffuser (Fig. 6(a)) are 0.5 m and 0.04 m respectively. The air supply temperature is 22 ℃. The droplet concentration (C) in the air supply process is 0, which is the filtered and purified circulating air or the mixed air in which the circulating air and outboard new air separately account for a certain proportion. There are 2 return vents. One is generated by the continuous air extraction of an exhaust fan in the restroom. A part of the air is expelled from the gap between the room and restroom. When *ACH* is 8, the proportion is about 30%, which means the air extraction amount is about 89.6 m^3/h and the length and height of the door gap are 0.9 m and 0.012 m respectively. Most of the remaining air is expelled from the main return vent which is on the ceiling of the cabin. The length and height of the main return vent are 0.4 m and 0.2 m respectively. The 2 return vents are both set under free outflow conditions. Besides, $\partial C/\partial \boldsymbol{n}=0$ is assumed and $\boldsymbol{n}$ is the exit normal direction, which means the concentration gradient of the droplet during the exhalation process is 0.

The hot box is utilized to represent person bodies of 2 passengers who take the sleeping gesture and its length, width and heights are 1.8 m, 0.4 m and 0.2 m respectively. The sensible heats gained from 2 bodies of passengers are both 76 W. Since this research does not consider the radiant heat exchange but only consider the convection heat exchange, according to the Reference[13], the convection heat exchange of human body should be set as half of the sensible heat, that is, 38 W. Considering that the cabin provides the accommodation for passengers in the evening, the cabin will not use other heat sources such as television and electric lamp which are usually turned off in the evening and all of the walls are assumed as possessing adiabatic boundary condition and zero concentration gradient boundary condition, i.e., $\partial T/\partial \boldsymbol{n}=0$ and $\partial C/\partial \boldsymbol{n}=0$; $\boldsymbol{n}$ is the normal direction of the wall.

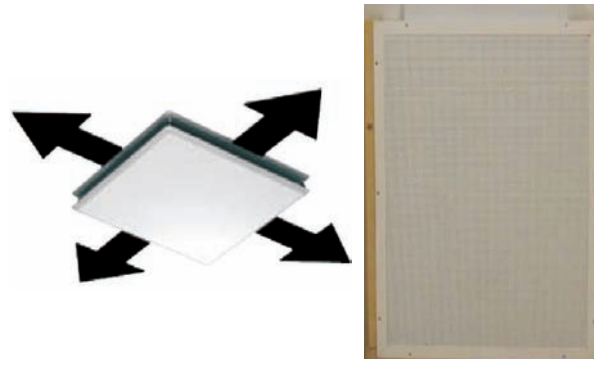

(a) Four-directional diffuser on ceiling

(b) Diffuser with porous structure for displacement ventilation

Fig.6 Diffusers

On the basis of case 1, instead of improving the ventilation mode, the case 2 increases the ventilation rates by 50%, which means the ACH is 12. The air extraction amount of passing through the door gap remains unchanged which still is 89.6 m^3/h.

The calculation physical models of case 3 and case 4 are shown in Fig. 7. Case 3 adopts the displacement ventilation mode and arranges the displacement ventilation air diffuser (Fig. 6(b)) in the position between the table and bed which is close to the floor. This diffuser possesses the porous structure and the ratio of effective area of vent to surface area

(height × width: 0.6 m × 0.4 m) is 1: 3. The momentum source method described in Section 1.2 is adopted to set inflow boundary condition of vent of this diffuser.

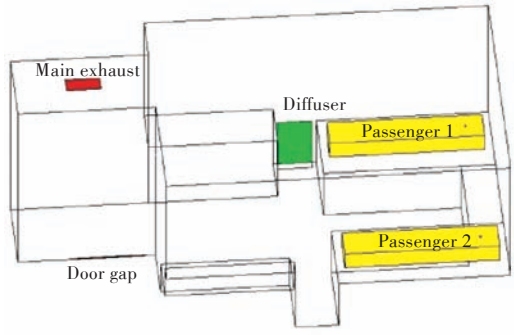

(a) Case 3

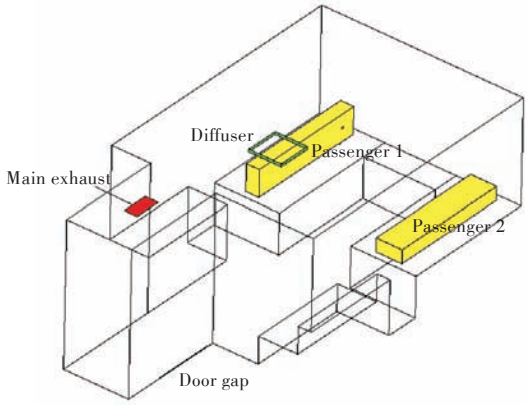

(b) Case 4

Fig.7 Computational physical models of cases 3 and 4

Case 4 researches the influences of sleeping gesture on the dispersion of droplet. In this case, the passenger 1 needs to face to passenger 2 and lies on his side. Other boundary conditions remain unchanged.

2.2 Boundary condition setting of coughing

Since the jet flow momentum of periodic air flow generated by human body breath through the nasal cavity is far less than that coughed by mouth, this research ignores the respiratory process of nasal cavity, that is, the disturbance of periodic air flow breathed through the nasal cavity to the air flow within the cabin. According to experimental measurement results[5, 14] of Gupta (Fig. 8), the distance between the centers of these 2 passengers′ mouths and the top of their heads is 0.2 m and the area is set as 4 cm^2 (2 cm × 2 cm). Coughing angle of passenger 1 is at a 30-degree angle downward to the normal direction of his mouth, and the temperature of coughing droplet is 33 ℃. Besides, the maximum speed of the pulse jet generated by coughing is about 9 m/s and the time of duration is about 0.4 s. Its time-dependent velocity curve is shown in Fig. 9 which is distributed based on Γ probability. For one cough, 10^6 droplets (diameter: 1 μm; volume: 0.69 L) will be erupted.

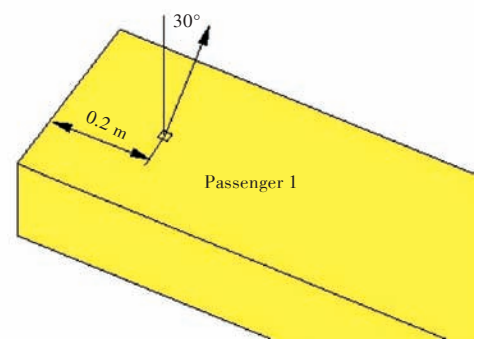

Fig.8 Location of mouth and coughing angle

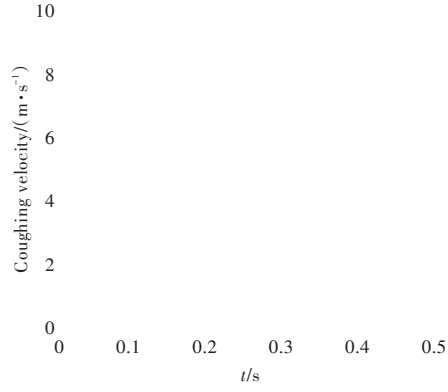

Fig.9 Velocity curve of coughing

This research firstly conducts the steady-state simulation for the air flow field of the cabin and uses this stimulation as the initial conditions of unsteady simulation. The cough boundary conditions of cases 1, 2 and 3 in Table 1 are all the same, while the cough angle in case 4 needs to change according to sleeping gesture of passenger and other boundary conditions of cough remain unchanged. The user-defined functions written based on the velocity curve in Fig. 9 are used as the velocity boundary condition of cough. Passenger 1 is assumed to cough once at the time zero (t = 0 s). Then his mouth is set as the velocity boundary condition within the time of 0–0.4 s. After 0.4 s, his cough stops and his mouth closes to be set as wall boundary condition. The mouth of passage 2 is set as wall boundary condition. Then the solution strategy of variable step size is adopted to further solve the coughing droplet transmission and dispersion process for a duration time of 1 350 s (the required time for three air changes in the cabin when ACH is 8) in the cabin.

In order to test the grid independence, unstruc-

tured grids (the grid cell numbers are 650 904, 108 4751 and 2 933 515) are applied in cases 1 and 3, and the local grid refinement is conducted in the mouth, other parts of the body, supply vent, main return vent and return vent of restroom door gap. The grid independence test indicates that when there are 1 084 751 grid cells, it will possess sufficient analysis accuracy and can be used to catch the turbulence within the cabin. The average value of $y+$ which is the non-dimensional value reflecting boundary layer thickness is greater than 15, which meets the application requirements of standard wall function of logarithmic layer. Cases 2–4 employ the same grid partition strategy.

3 Results analysis

In order to evaluate the exposed infection risk of passenger 2 for inhaling droplet, it is quite necessary to monitor the droplet concentration in his breathing space area close to his face and establish a breathing zone of 0.3 m × 0.3 m × 0.3 m, as shown in Fig. 10.

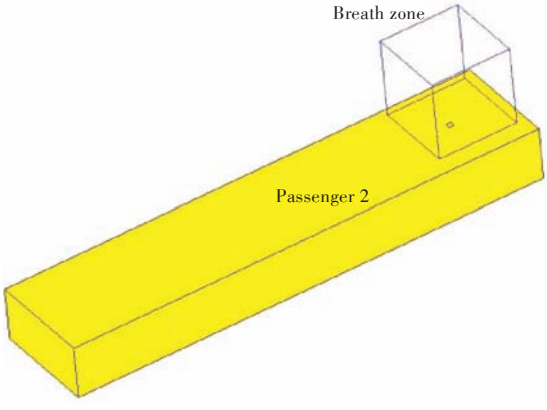

Fig.10 Breathing zone near the face of passenger 2

3.1 Droplet concentration in breathing zone of passenger 2

The time-dependent changing curves of droplet concentration of cases 1, 2 and 3 in breathing zone of passenger 2 are shown in Fig. 11. All concentration values adopt the normalized maximum concentration value in 3 cases. The results show that case 1 possesses the maximum droplet concentration as a whole, while case 2 takes the second place. This is because case 2 increases the fresh air volume so that it can dilute the droplet concentration in the cabin more quickly. The air-stirring effects in the cabin are more obvious, so that it can bring the droplet coughed by passenger 1 to breathing zone of passenger 2 more quickly. Although it reaches the peak value of droplet concentration in the breathing zone earlier than case 1, its droplet concentration drops rapidly because the fresh air constantly participates in the stirring and dilution process. From an overall perspective, compared to cases 1 and 2, case 3 possesses the minimum droplet concentration in the breathing zone, which indicates that not increasing the ventilation rates but changing the ventilation mode (change the mixed ventilation mode into displacement ventilation mode) can exert better effects on controlling the droplet concentration in the breathing zone than only increasing the ventilation rates.

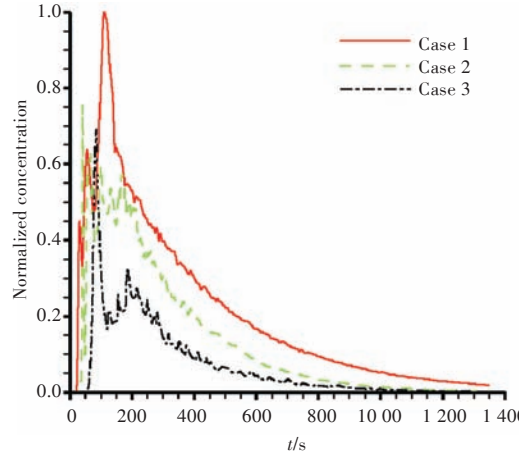

Fig.11 Droplet concentration curves in the breathing zone of passenger 2

The droplet concentration distribution on the vertical line between the mouth center of passenger 2 and the ceiling is investigated. When t is 105 s, the changing curve of concentration is as shown in Fig. 12. All concentration values adopt the normalized maximum concentration value in 3 cases. The results show that when t is 105 s, case 1 has not been evenly stirred and its droplet concentration value within the breathing zone (z = 0.8–1.1 m) is much higher than that at the top of the cabin. However, since case 2 increases the ventilation rates, it is evenly stirred approximately. Case 3 forms a concentration gradient

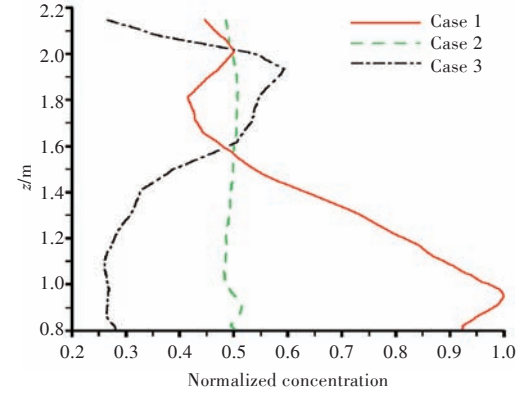

Fig.12 Droplet concentration curves in an investigated line (t=105 s)

in the vertical direction and its droplet concentration value within the breathing zone is far less than that at the top of the cabin. This is because the displacement ventilation mode generates the stratified air flow in the cabin.

Cases 1, 2 and 3 all successfully catch the thermal plume generated by human body. Fig. 13 displays thermal plumes at the waist of the body of cases 1 and 3 which are generated by heat convection between the air and heating human body when t is 0 s.

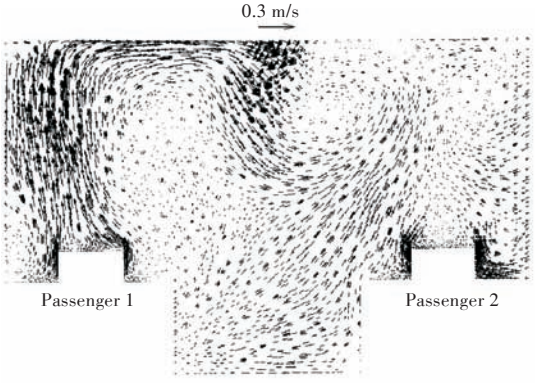

(a) Case 1

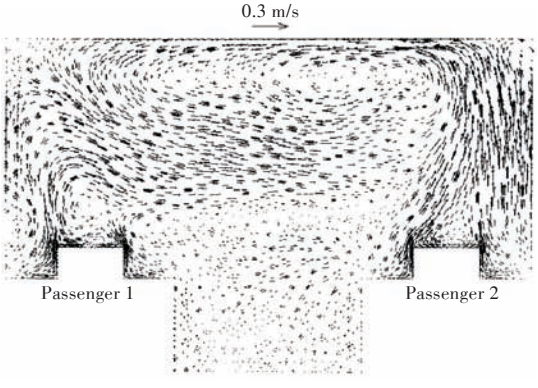

(b) Case 3

Fig.13 Thermal plumes generated by person bodies

3.2 Dispersion process of droplet

The data of case 1 are utilized to illustrate the droplet dispersion process. Fig. 14 displays the droplet concentration distribution at the time that passenger 1 just stops his cough (t = 0.4 s) and the concentration value uses the coughing normalized initial droplet concentration value (1.45×10^9 droplets/m^3). It can be seen that when t is 0.4 s, the distribution of droplet concentration is consistent with the angle of cough jet without dispersion. Fig. 15 is a three-dimensional iso-surface figure of dispersed droplet concentration. The value of droplet concentration is 2.5×10^{-5} times the initial value of coughing droplet concentration. The results indicate that the droplet presents an unsteady and nonuniform spatial distri-

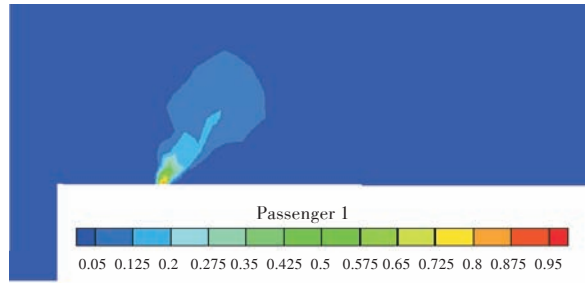

Fig.14 Droplet concentration distribution when coughing is finished (t=0.4 s)

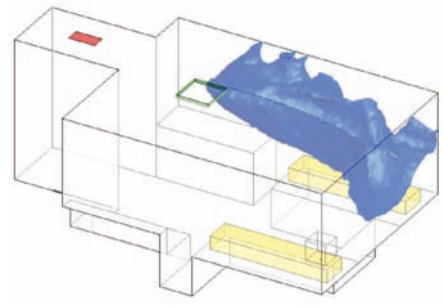

(a) t=21 s

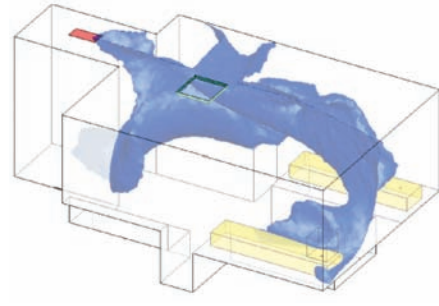

(b) t=51 s

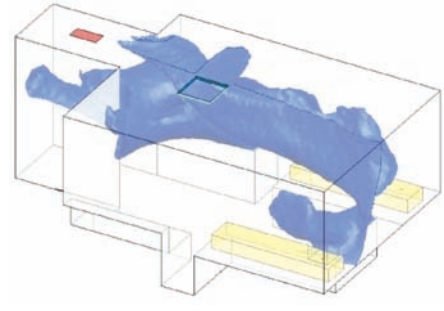

(c) t=75 s

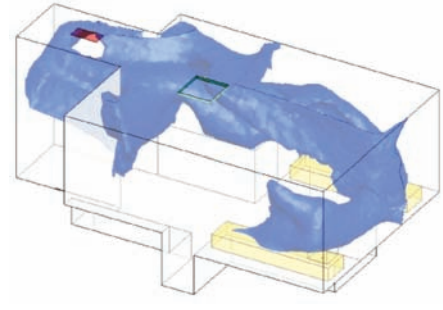

(d) t=125 s

Fig.15 Iso-surfaces of dispersed droplet concentration (the normalized concentration is 2.5×10^{-5} compared with the concentration of the instantaneous coughed air)

bution. When t is 21 s, the droplet cloud has not reached the breathing zone of passenger 2. When t equals to 51 s, 75 s and 125 s, the droplet cloud of this concentration value all reach the breathing zone. This is consistent with the relatively high droplet concentration of case 1 in Fig. 11.

3.3 Inhaled dose of passenger 2

Compared to the droplet concentration in breathing zone of passenger 2, inhaled dose of droplet plays a more important role in evaluating the risk of catching respiratory diseases. The computational formula of inhaled dose (ID) is as follows:

$$ID = q\int_{t=0}^{t} C(t)\mathrm{d}t \tag{3}$$

where $C(t)$ refers to the droplet concentration in breathing zone of passenger 2; t represents the time; q is the respiratory rate of passenger, which is set as 0.48 m^3/h[15].

Fig. 16 compares different inhaled droplet dose of the passenger 2 within the duration time of 1 350 s in cases 1, 2 and 3. All values of inhaled dose adopt the normalized maximum inhaled dose in the three cases. Case 1 possess the maximum inhaled dose and the inhaled doses of case 2 and case 3 account for 64.7% and 32.3% of inhaled dose of case 1 respectively. The results show that only changing the ventilation mode can make the inhaled dose be about one third of the original value and it will be half of inhaled dose when increasing 50% of the ventilation rate.

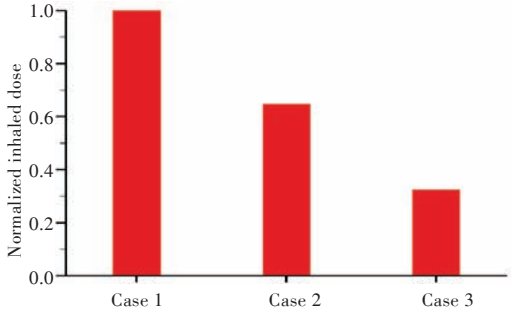

Fig.16 Inhaled droplet dose of passenger 2

3.4 Dilution effect analysis of fresh air

Fig. 17 compares the variation tendency of average droplet concentration in the whole cabin in cases 1, 2 and 3 to explore the dilution effects of the fresh air supplied by supply vent. All concentration values adopt the normalized maximum averaged concentration value in 3 cases. After passenger 1 sprays 10^6 droplets into the air environment of the cabin by coughing, the average droplet concentrations of the cabin in cases 1, 2 and 3 are all the same and all begin to decrease after 40 s, which indicates that some droplets start to be exhausted from the main return vent and door gap return vent between room and restroom. In these 3 cases, the reduction trend of averaged droplet concentration obeys exponential distribution. However, their reduction velocity is not the same. The reduction velocity of case 1 is the slowest and those of cases 2 and 3 are basically the same. This indicates that the method of only changing the ventilation mode can obtain the similar controlling effects to the method of only increasing 50% of the ventilation rate.

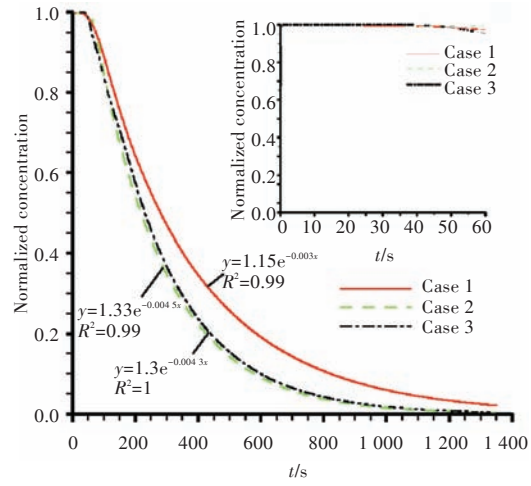

Fig.17 Averaged droplet concentration in the cabin

When ACH is 8, for case 1, after 450 s, 900 s and 1 350 s, the ratios of the remaining droplets amount to the coughing droplets amount are 25.8%, 6.9% and 1.8% respectively. For case 3, the proportions of the remaining droplets amount are 16.5%, 2.4% and 0.3% respectively. When ACH is 12, for case 2, after 300 s, 600 s and 900 s, the proportions of the remaining droplets amount are 30.1%, 7.9% and 2.6% respectively. The results indicate that the mixed ventilation mode needs three air changes to generally empty the droplet generated by a cough, while the displacement ventilation mode needs only two.

4 Discussions

When passenger 1 adopts side lying facing to passenger 2, the effects on the droplet concentration and inhaled dose in breathing zone of passenger 2 are investigated by case 4. Fig. 18 shows the time-dependent changing curves of droplet concentration of cases 1 and 4 in breathing area of passenger 2. All concentration values adopt the normalized maximum concentration value in these 2 cases. The results show that the maximum concentration value of case

4 is about 2.5 times higher than that of case 1, while the inhaled dose of case 4 is only 29.5% higher than that of case 1. Besides, the time when the peak value is reached is earlier, this is because when passenger 1 (side lying facing to passenger 2) coughs, the droplet is much easier dispersed to breathing zone of passenger 2 (by comparing Fig. 19 with Fig. 15(b), it can be seen that the droplet cloud basically cover the whole breathing zone of passenger 2). Problems such as the controlling effects of side lying of passenger 1 under the situation of increasing ventilation rates or the displacement ventilation mode and other sleeping gestures still need to be further studied.

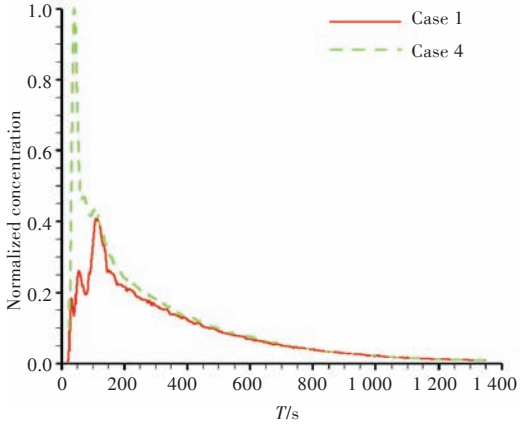

Fig.18 Droplet concentration curves in the breathing zone of passenger 2 (cases 1 and 4)

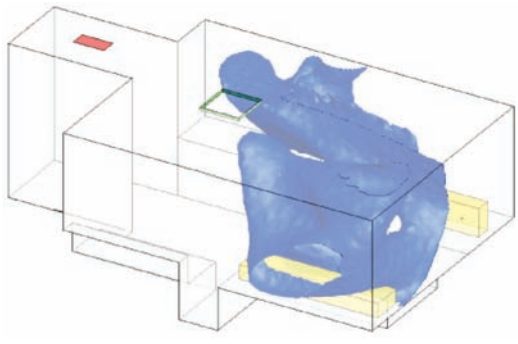

Fig.19 Iso-surface of dispersed droplet concentration (case 4, t=51 s, the normalized concentration is 2.5×10^{-5} compared with the concentration of the instantaneous coughed air)

For the convenience of comparing simulation results, the displacement ventilation mode adopted by case 3 uses the same air supply temperature (22 ℃) and air supply volume as those of case 1. If the displacement ventilation mode can employ a lower air supply temperature, it will have better controlling effects on the droplet concentration. Besides, because of the storey height limits of the low-rise cabin, the flow stratification effects of the cabin are inferior to those of the space with high storey height. In addition, the displacement ventilation diffuser is usually very large and leads to difficult arrangement in the narrow cabin. As a result, the displacement ventilation design aiming at cabins of different storey heights, diversified air supply parameters and geometrical arrangements need to use CFD method to further deepen its research. Moreover, case 2 increases 50% of the ventilation rate, which to some extent exerts effects of diluting the droplet concentration. However, this method will increase the energy consumption and affect the operating profits of cruise ships. At the same time, the capacity limitation of ventilation and air conditioning system of ships may not meet the requirements of increasing 50% of the ventilation rate.

5 Conclusions

This paper utilizes CFD method solving URANS and Eulerian model to conduct the numerical simulation for the droplet transmission and dispersion process coughed by an infected passenger accommodated in an enclosed cabin on a cruise ship. It investigates the controlling effects of increasing the ventilation rate, changing the ventilation mode and sleeping gestures of passenger son reducing the droplet concentration. The RNG $k-\varepsilon$ turbulence model and Eulerian model verified by experimental results of similar flowing phenomenon, the cough boundary conditions input by measurement results and grid independence analysis can ensure the dependability of calculation results. The results of relevant research are as follows:

1) Increasing the ventilation rates of mixed ventilation mode and the displacement ventilation mode can both effectively control the droplet concentration and inhaled dose in the breathing zone of passengers who are in a healthy state, but the latter has better effect.

2) Three air changes are needed to empty the droplet in the cabin under the mixed ventilation mode, while the displacement ventilation mode needs only two.

3) Under the mixed ventilation mode and displacement ventilation mode, the reduction of average droplet concentration in the cabin obeys exponential distribution.

4) The sleeping gestures of the passenger have big influences on the peak droplet concentration and inhaled dose in the breathing zone.

This research not only offers a quantitative understanding for the droplet dispersion process in enclosed cabin of ship and the spread of airborne infec-

tious diseases but also provides references for optimizing and improving the design of ventilation and air conditioning system as well as air flow design. This method can be used for the transportation stimulation of other gaseous contaminants and small granules and quantitative risk assessment of respiratory diseases.

References

[1] Cruise Lines International Association Inc. The state of the cruise industry in 2014: global growth in passenger numbers and product offerings[EB/OL]. (2014-1-16)[2014-9-1]. http://www.cruising.org/vacation/news/press_releases / 2014 /01/state-cruise-industry-2014-global-growth-passenger-numbers-and-product-o.

[2] PEAKE D E, GRAY C L, LUDWIG M R, et al. Descriptive epidemiology of injury and illness among cruise ship passengers [J]. Annals of Emergency Medicine, 1999, 33(1): 67-72.

[3] NICAS M, NAZAROFF W W, HUBBARD A. Toward understanding the risk of secondary airborne infection: emission of respirable pathogens [J]. Journal of Occupational and Environmental Hygiene, 2005, 2(3): 143-154.

[4] HE Q B, NIU J L, GAO N P, et al. CFD study of exhaled droplet transmission between occupants under different ventilation strategies in a typical office room [J]. Building and Environment, 2011, 46(2): 397-408.

[5] GUPTA J K, LIN C H, CHEN Q Y. Transport of expiratory droplets in an aircraft cabin [J]. Indoor Air, 2011, 21(1): 3-11.

[6] ZHU S W, SREBRIC J, SPENGLER J D, et al. An advanced numerical model for the assessment of airborne transmission of influenza in bus microenvironments [J]. Building and Environment, 2011, 47: 67-75.

[7] ZHANG L, LI Y G. Dispersion of coughed droplets in a fully-occupied high-speed rail cabin [J]. Building and Environment, 2012, 47: 58-66.

[8] ZHAO B, CHEN C, TAN Z C. Modeling of ultrafine particle dispersion in indoor environments with an improved drift flux model [J]. Journal of Aerosol Science, 2009, 40(1): 29-43.

[9] CHEN Q. Comparison of different k-ε models for indoor air flow computations [J]. Numerical Heat Transfer, Part B: Fundamentals: An International Journal of Computation and Methodology, 1995, 28(3): 353-369.

[10] YUAN X, CHEN Q, GLICKSMAN L R, et al. Measurements and computations of room airflow with displacement ventilation [J]. ASHRAE Transactions, 1999, 105(1): 340-352.

[11] CHEN Q, MOSER A. Simulation of a multiple-nozzle diffuser[C]//Proceeding of the 12th AIVC Conference on Air Movement and Ventilation Control within Buildings. Ottawa, Canada, 1991.

[12] Shanghai Merchant Ship Design & Research Institute. Air-conditioning and ventilation of accommodation spaces on board ships-Design parameter and method of calculations: GB/T 13409-1992[S]. Beijing: Standards Press of China, 1992 (in Chinese).

[13] QIAN H, LI Y. Removal of exhaled particles by ventilation and deposition in a multibed airborne infection isolation room[J].Indoor Air,2010,20(4): 284-297.

[14] GUPTA J K, LIN C H, CHEN Q. Flow dynamics and characterization of a cough [J]. Indoor Air, 2009, 19(6): 517-525.

[15] CHEN S C, CHANG C F, LIAO C M. Predictive models of control strategies involved in containing indoor airborne infections [J].Indoor Air,2006,16(6): 469-481.

通风模式对住舱人员咳嗽液珠扩散过程的影响

郑立捷[1], 许建[1], 吴方良[1], 徐文涛[1], 龙正伟[2]

1 中国舰船研究设计中心,湖北 武汉 430064

2 天津大学 环境科学与工程学院,天津 300072

摘　要: 针对邮轮上呼吸道疾病发病率高及缺乏相关定量研究的现状,采用计算流体力学方法分析了游客在密闭住舱内因为咳嗽产生的液珠在空气中的传播扩散过程,对空气流动采用非定常雷诺平均纳维—斯托克斯方程求解,对液珠扩散采用欧拉模型求解,计算工况考察了改变通风模式和加大通风量等方式降低液珠浓度的控制效果。研究结果表明:加大通风量在置换通风模式比混合通风模式下可更好地控制液珠的扩散,混合通风模式需要3次换气才能把住舱内的液珠基本排空,而置换通风模式仅需2次换气,且住舱内液珠平均浓度的下降服从指数分布。此外,游客睡姿对呼吸区域内液珠浓度峰值和吸入剂量有较大影响。

关键词: 邮轮住舱; 液珠扩散; 通风模式; 数值模拟